



Published in final edited form as:

Chem Commun (Camb). 2017 June 29; 53(53): 7349–7352. doi:10.1039/c7cc03455e.

Cell-sized mechanosensitive and biosensing compartment programmed with DNA

Sagardip Majumder^{†,a}, Jonathan Garamella^{†,b}, Ying-Ling Wang^c, Maxwell DeNies^d, Vincent Noireaux^{*,b}, and Allen P. Liu^{*,a,d}

^aDepartment of Mechanical Engineering, University of Michigan, Ann Arbor, Michigan, USA

^bDepartment of Physics and Astronomy, University of Minnesota, Minneapolis, Minnesota, USA

^cDepartment of Biomedical Engineering, National Cheng Kung University, Tainan, Taiwan

^dCellular and Molecular Biology Program, University of Michigan, Ann Arbor, Michigan, USA

Abstract

The bottom-up construction of cell-sized compartments programmed with DNA that are capable of sensing the chemical and physical environment remains challenging in synthetic cell engineering. Here, we construct mechanosensitive liposomes with biosensing capability by expressing the *E. coli* channel MscL and a calcium biosensor using cell-free expression.

Cell-free expression (CFE) has been recently reshaped into a highly versatile technology applicable to an increasing number of research areas¹. The new generation of DNA-dependent cell-free transcription-translation systems (TXTL) has been engineered to address applications over a broad spectrum of engineering and fundamental disciplines, from synthetic biology to biophysics and chemistry^{2–4}. Modern TXTL platforms are used for medicine and biomolecular manufacturing, such as the production of vaccine and therapeutics^{5, 6}. By performing non-natural chemistries^{3, 7, 8}, the TXTL technology has been improved to expand the molecular repertoire of biological systems. Because the time for design-build-test cycle is dramatically reduced, TXTL has become a powerful platform to rapidly prototype genetic programs *in vitro*, from testing single regulatory elements to recapitulating metabolic pathways⁹. Remarkably, the new TXTL systems have also been prepared so as to work at many different scales and in different experimental settings. As such, TXTL reactions can be carried out in volumes spanning more than twelve orders of magnitudes, from bulk reactions to microfluidics and artificial cell systems^{2, 10–13}.

The bottom-up construction of synthetic cells that recapitulates gene expression has become an effective means to characterize biological functions in isolation and to prototype cell-sized compartments as chemical bioreactors for applications in biotechnology^{14, 15}. In particular, engineering artificial cells integrating active membrane functions is critical to

^{*}Corresponding authors: V.N.: noireaux@umn.edu, A.P.L.: allenliu@umich.edu.

[†]S.M. and J.G. contributed equally to this work.

Electronic Supplementary Information (ESI) available: Materials and methods and Supplementary Figures. See DOI: 10.039/x0xx00000x

develop mechanically robust compartments capable of sensing the physical and chemical environment. Such undertaking, however, remains challenging as only a few synthetic cell systems loaded with executable genetic information and harboring membrane sensors have been achieved¹⁶. In this work, we construct synthetic cells capable of responding to the osmotic pressure by expressing the *E. coli* mechanosensitive membrane protein MscL using a TXTL system encapsulated into synthetic liposomes. Using the calcium sensitive reporter G-GECO, we demonstrate that the osmotic pressure and calcium intake can be detected simultaneously, at different concentrations of the divalent ion. TXTL is carried out with a highly versatile all *E. coli* cell-free toolbox based on the endogenous transcription machinery (*E. coli* core RNA polymerase and sigma factor 70, $\sigma 70$). We characterize the channel function by monitoring the fluorescence of G-GECO and the leak of polymers of various sizes. Our novel approach expands the functional capabilities of encapsulated cell-free TXTL reactions and demonstrates, for the first time, that synthetic cell systems with biosensing interfaces can be achieved by directly expressing membrane proteins inside liposomes.

Our general methodology is to encapsulate TXTL reactions within phospholipid vesicles as a versatile platform that recapitulates *in vitro* transcription-translation for producing proteins that endow biosensing and molecular transport properties to the vesicles (Fig. 1A). DNA-based cell-free protein synthesis inside liposomes links the information contained in the DNA to the phenotype of synthetic cells in a reduced environment suitable for isolation and characterization of cellular functions. Like a complex chemical reaction that can be broken down to elementary processes, biochemical reactions based on genetic circuits can also be constructed to control rates of protein production. Such settings are conveniently adjusted in TXTL by either choosing the appropriate plasmids stoichiometry and circuit architectures, or by calibrating the strength of promoters and ribosome binding sites². In this work, we used two different genetic circuit schemes to produce proteins of interests (Fig. 1B). In the first scheme, the endogenous *E. coli* core RNA polymerase $\sigma 70$ drives the transcription of downstream coding sequence through the constitutive promoter P70a². Our second scheme is a transcriptional activation cascade where P70a/ $\sigma 70$ drives the expression of sigma factor 28 ($\sigma 28$) that is required for subsequent expression from a P28a promoter sequence specific to $\sigma 28$. We first used the reporter protein deGFP to characterize the circuit functions and features². deGFP is a slightly modified version of eGFP with identical fluorescence properties. Both schemes were then used to express G-GECO, a genetically encoded green fluorescence protein whose fluorescence depends on calcium concentration¹⁷, and the *E. coli* mechanosensitive channel of large conductance (MscL) for biosensing and incorporating a membrane-active property, respectively.

We first performed bulk reactions (10 μ l reactions) and compared deGFP expression kinetics of the single-step circuit vs. the transcriptional activation cascade circuit. As expected, the requirement for $\sigma 28$ to drive expression of deGFP in the transcriptional activation resulted in a delay in deGFP expression compared to the single-step circuit (Fig 2A). The delay observed for the cascade, on the order of 15 minutes, corresponded to the amount of time necessary for the synthesis of $\sigma 28$. The bulk reaction persisted for many hours and deGFP production began to slow down after 8 hours and reached a plateau after 10 hours. The time course observed in these experiments is typical for TXTL reactions where protein synthesis

using the transcriptional activation cascade, the delay in MscL expression (about 15 minutes) is advantageous because it corresponds to the amount of time needed to prepare the liposomes. We first expressed MscL-eGFP to visualize MscL localization. We observed the accumulation of MscL-eGFP at the membrane over time as expected (Fig. S2). In order to test MscL function, we developed a simple dye-leakage assay where TRITC-labeled dextrans of different molecular weight (3, 10, and 70 kDa) and TXTL reaction producing wild type MscL were co-encapsulated using the emulsion method to make liposomes (Fig. 3A). We expressed the native MscL without a fluorescent protein tag as MscL fusion proteins have a higher activation tension threshold¹⁸. In our experiments, we relied on the osmotic pressure from a hypo-osmotic feeding solution (~630 mOsm) relative to the encapsulated TXTL reaction (~700 mOsm). In the absence of MscL expression, 5 μ M of 3,000 Da TRITC-dextran remained encapsulated in the vesicle after 2 hours (Fig. 3B). In contrast, MscL expression led to dye-leakage after 20–30 minutes. When a larger 10,000 Da TRITC-dextran was used, we observed complete dye-leakage after 60 minutes in MscL-expressing vesicles (Fig. S3A and S3B). Larger dextran molecules at 70,000 Da were completely retained after 120 minutes with or without MscL expression (Fig. S3C), with no leakage observed after 12 hours of incubation (data not shown). We also tested the leakage of two proteins, deGFP (27 kDa) and BSA-TRITC (60 kDa). Both were also completely retained inside the liposomes in MscL-expressing vesicles after 2 hours of incubation (Fig. S3D). No leakage was observed after overnight incubation (data not shown).

Our next challenge was to use a genetically-encoded reporter and demonstrate that we can couple a mechanical input to biosensing. We cloned the genetically-encoded calcium ion (Ca^{2+}) biosensor G-GECO that is composed of a circularly permuted GFP fused to the calmodulin (CaM)-binding region of myosin light chain kinase M13 at its N-terminus and CaM at its C-terminus²¹. G-GECO is dim in the absence of Ca^{2+} and bright when bound to Ca^{2+} with a Ca^{2+} -dependent fluorescence increase of ~23–26 fold (Fig. 4A)⁷. We cloned G-GECO under the P70a promoter and verified that it can sense Ca^{2+} in a plate reader assay (Fig. S4A). To eliminate traces of Ca^{2+} present in TXTL reactions estimated to be up to 1 mM Ca^{2+} , we added 1 mM EGTA to the TXTL reactions so that G-GECO can report an increase in calcium level when externally added to the reactions. Both G-GECO and MscL-eGFP can be produced together in a single TXTL reaction, as shown by the increased fluorescence level by G-GECO after adding 1 mM Ca^{2+} at 120 minutes after TXTL started (Fig. S4B).

To create mechanosensitive-biosensing vesicles, we employed double emulsion templated vesicles generated by droplet microfluidics^{22, 23}. We have previously used this approach and showed that small molecules from the feeding solution can enter encapsulated vesicles containing integrated synthesis, assembly, and translation (iSAT) reactions¹⁰. We have also shown that Ca^{2+} can enter a double emulsion droplet with an ultrathin oil layer as the middle phase when the droplet is under hypo-osmotic shock²⁴. However, Ca^{2+} as a charged ion cannot cross a lipid bilayer. When G-GECO was expressed in the presence of 1.5 mM Ca^{2+} inside a vesicle, fluorescence was readily detected after 90 minutes, demonstrating that G-GECO can be used to detect increased calcium concentration in an artificial cell (Fig. 4B). As expected, if Ca^{2+} is added to the outside (at 10 mM) of G-GECO expressing vesicle, no G-GECO fluorescence was observed because Ca^{2+} is impermeable to phospholipid

membrane (Fig. S5A). However, addition of a calcium ionophore A23187 allowed rapid entry of Ca^{2+} and G-GECO fluorescence was readily observed in as little as 10-minute post A23187 addition (Fig. S5B).

To couple mechanical input to sensing the external environment, we co-expressed G-GECO (under P70a promoter) and MscL (under P28a promoter) in TXTL for 2 or 3 hours and then encapsulated the reaction into double emulsion templated vesicles. Under iso-osmotic condition, we did not observe G-GECO fluorescence for over 10 hours, our longest observation time point (Fig. 4Ci). In contrast, hypo-osmotic condition of ~ 100 mOsm osmotic difference between inside and outside the vesicle robustly led to an increase in G-GECO fluorescence as Ca^{2+} was able to enter the lipid bilayer membrane through MscL (Fig. 4Cii). To our knowledge, this is the first demonstration of an AND-gate composed of a mechanical input (i.e. hypo-osmotic pressure) and an external chemical input (i.e. Ca^{2+}) that lead to a specific fluorescence response. The synthetic cell system is also sensitive to the concentration of calcium added to the external solution (Fig. 4D and Fig. S6). The detection time for calcium intake was as short as 20 minutes.

In summary, we have generated a DNA-programmed cell-sized artificial cell that senses osmotic pressure and external calcium concentration. We demonstrated two different circuit architectures for TXTL that exhibit different reaction kinetics that are preserved across length scale from bulk reactions to micron-sized encapsulated droplets or vesicles. The ability to endow artificial cells with mechanosensitive functions to sense external small molecules using genetically-encoded biosensors allows for rapid sensing, rather than relying on fluorescence reporter synthesis using chemical inducers that most studies have used^{25, 26}. Recapitulating TXTL for synthetic cell engineering can be used for reconstituting cellular processes and functions²⁷. It can also serve as a powerful platform for chemical applications, such as biosensing and novel synthetic pathways for chemicals.

Supplementary Material

Refer to Web version on PubMed Central for supplementary material.

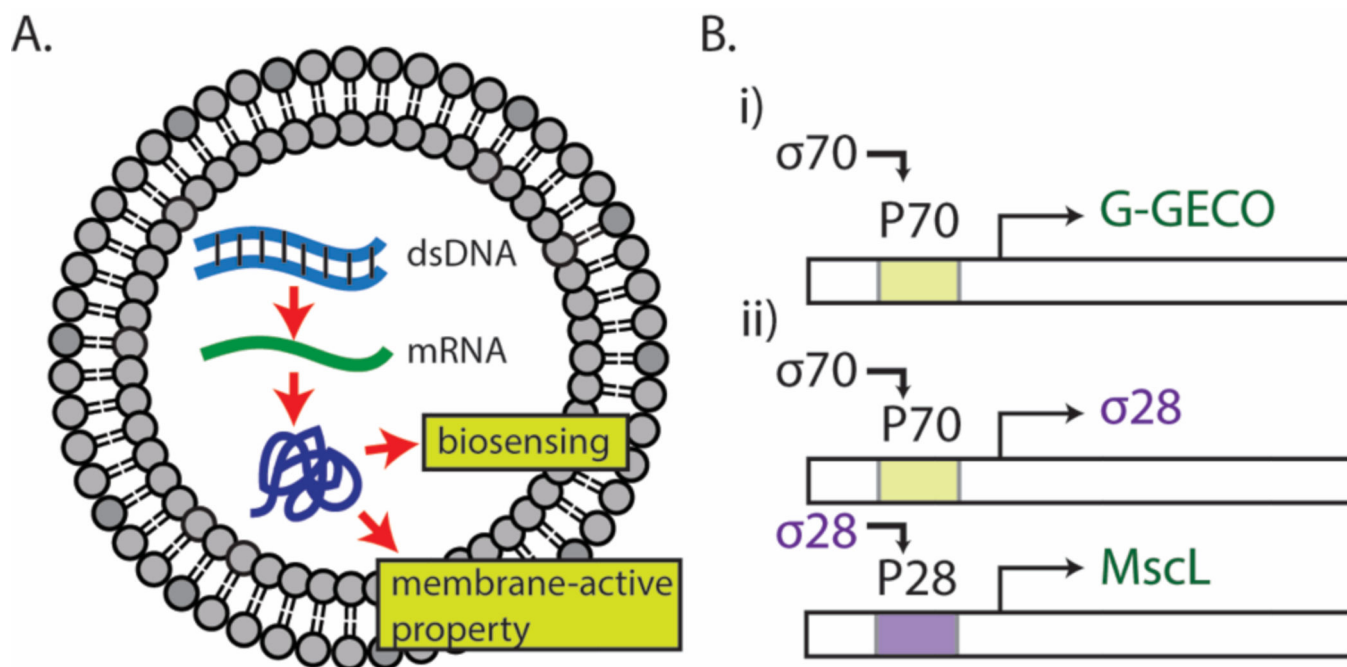
Acknowledgments

We thank Takanari Inoue (Johns Hopkins University) for providing the G-GECO plasmid. This work is supported by the NSF MCB-1612917 to A.P.L. and MCB-1613677 to V.N, the NIH Director's New Innovator Award DP2 HL117748-01 to A.P.L., and the Human Frontier Science Program grant number RGP0037/2015 to V.N.. Y.-L.W. acknowledges support from the Global Networking Talent 3.0 Plan by Medical Device Innovation Center, NCKU. M.D. is supported by a NSF graduate fellowship.

Notes and references

1. Carlson ED, Gan R, Hodgman CE, Jewett MC. *Biotechnol Adv.* 2012; 30:1185–1194. [PubMed: 22008973]
2. Garamella J, Marshall R, Rustad M, Noireaux V. *ACS Synth Biol.* 2016; 5:344–355. [PubMed: 26818434]
3. Iwane Y, Hitomi A, Murakami H, Katoh T, Goto Y, Suga H. *Nat Chem.* 2016; 8:317–325. [PubMed: 27001726]
4. Tayar AM, Karzbrun E, Noireaux V, Bar-Ziv RH. *Nature Physics.* 2015; 11:1037–1041.

5. Pardee K, Slomovic S, Nguyen PQ, Lee JW, Donghia N, Burrill D, Ferrante T, McSorley FR, Furuta Y, Vernet A, Lewandowski M, Boddy CN, Joshi NS, Collins JJ. *Cell*. 2016; 167:248–259. e212. [PubMed: 27662092]
6. Ng PP, Jia M, Patel KG, Brody JD, Swartz JR, Levy S, Levy R. *Proc Natl Acad Sci U S A*. 2012; 109:14526–14531. [PubMed: 22875703]
7. Chemla Y, Ozer E, Schlesinger O, Noireaux V, Alfonta L. *Biotechnol Bioeng*. 2015; 112:1663–1672. [PubMed: 25753985]
8. Hong SH, Kwon YC, Jewett MC. *Front Chem*. 2014; 2:34. [PubMed: 24959531]
9. Takahashi MK, Hayes CA, Chappell J, Sun ZZ, Murray RM, Noireaux V, Lucks JB. *Methods*. 2015; 86:60–72. [PubMed: 26022922]
10. Caschera F, Lee JW, Ho KK, Liu AP, Jewett MC. *ChemCommun (Camb)*. 2016; 52:5467–5469.
11. Noireaux V, Libchaber A. *Proc Natl Acad Sci U S A*. 2004; 101:17669–17674. [PubMed: 15591347]
12. Karzbrun E, Tayar AM, Noireaux V, Bar-Ziv RH. *Science*. 2014; 345:829–832. [PubMed: 25124443]
13. Ho KK, Lee JW, Durand G, Majumder S, Liu AP. *PLoS One*. 2017; 12:e0174689. [PubMed: 28358875]
14. Pohorille A, Deamer D. *Trends Biotechnol*. 2002; 20:123–128. [PubMed: 11841864]
15. Fujii S, Matsuura T, Sunami T, Nishikawa T, Kazuta Y, Yomo T. *Nat Protoc*. 2014; 9:1578–1591. [PubMed: 24901741]
16. Hamada S, Tabuchi M, Toyota T, Sakurai T, Hosoi T, Nomoto T, Nakatani K, Fujinami M, Kanzaki R. *Chem Commun (Camb)*. 2014; 50:2958–2961. [PubMed: 24509495]
17. Zhao Y, Araki S, Wu J, Teramoto T, Chang YF, Nakano M, Abdelfattah AS, Fujiwara M, Ishihara T, Nagai T, Campbell RE. *Science*. 2011; 333:1888–1891. [PubMed: 21903779]
18. Cox CD, Bae C, Ziegler L, Hartley S, Nikolova-Krstevski V, Rohde PR, Ng CA, Sachs F, Gottlieb PA, Martinac B. *Nat Commun*. 2016; 7:10366. [PubMed: 26785635]
19. Lee LM, Liu AP. *Lab Chip*. 2015; 15:264–273. [PubMed: 25361042]
20. Heureaux J, Chen D, Murray VL, Deng CX, Liu AP. *Cell Mol Bioeng*. 2014; 7:307–319. [PubMed: 25606062]
21. Su S, Phua SC, DeRose R, Chiba S, Narita K, Kalugin PN, Katada T, Kontani K, Takeda S, Inoue T. *Nat Methods*. 2013; 10:1105–1107. [PubMed: 24056873]
22. Ho KK, Murray VL, Liu AP. *Methods Cell Biol*. 2015; 128:303–318. [PubMed: 25997354]
23. Utada AS, Lorenceau E, Link DR, Kaplan PD, Stone HA, Weitz DA. *Science*. 2005; 308:537–541. [PubMed: 15845850]
24. Ho KK, Lee LM, Liu AP. *Sci Rep*. 2016; 6:32912. [PubMed: 27610921]
25. Shin J, Noireaux V. *ACS Synth Biol*. 2012; 1:29–41. [PubMed: 23651008]
26. Siuti P, Yazbek J, Lu TK. *Nat Biotechnol*. 2013; 31:448–52. [PubMed: 23396014]
27. Liu AP, Fletcher DA. *Nat Rev Mol Cell Biol*. 2009; 10:644–650. [PubMed: 19672276]

**Fig. 1.**

Schematics of protein synthesis in liposomes and gene circuits. (A) dsDNA is transcribed into mRNA, which is then translated to a biosensing fluorescent reporter protein (G-GECO) and a mechanosensitive membrane-active protein (MscL). (B) Gene circuits used in this work. (i) The *E. coli* housekeeping transcription factor sigma 70 activates the promoter P70a. (ii) The sigma 28 cascade requires the expression of sigma 28 protein, expressed through the P70a promoter. The sigma 28 transcription factor activates the corresponding promoter P28a.

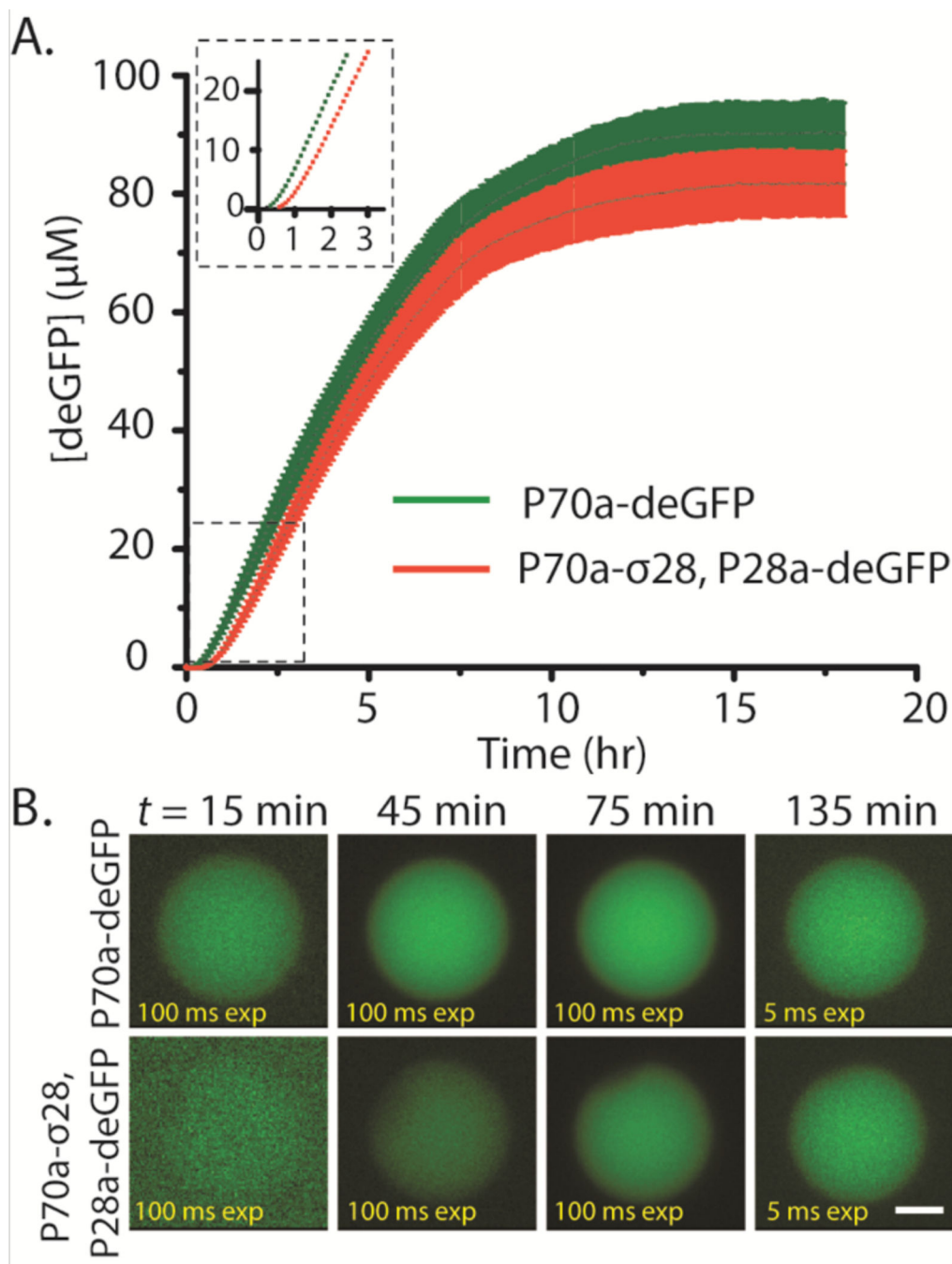


Fig. 2. deGFP synthesis in bulk reactions, single emulsions, and liposomes. (A) Kinetics of expression. Plasmid P70a-deGFP fixed at 5 nM, P70a-S28 fixed at 0.2 nM, and P28a-deGFP fixed at 5 nM. Inset: 0–3 hours magnified. (B) deGFP synthesis in liposomes using both the P70a plasmid and P28a cascade. Scale bar: 5 μm .

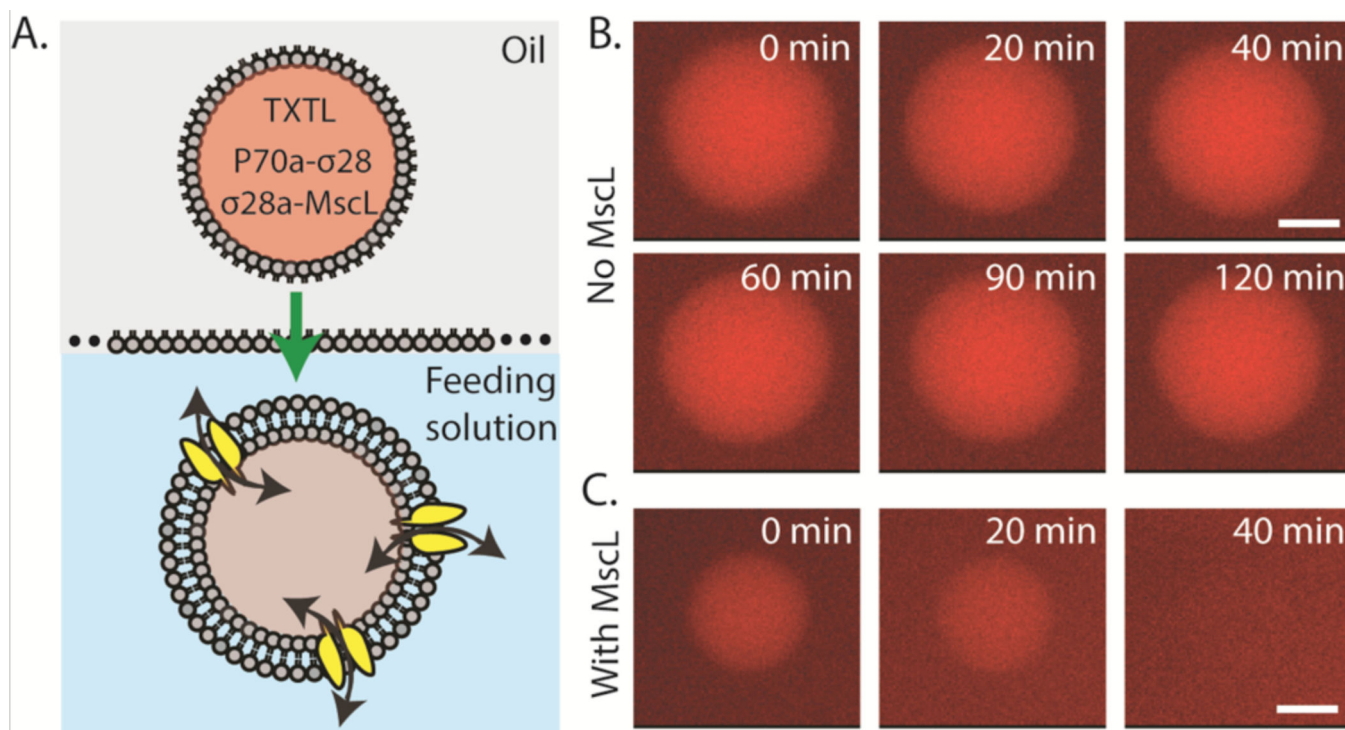


Fig. 3.

Leakage of a 3 kDa TRITC-dextran in liposomes in the absence or presence of MscL. (A) Schematic of the encapsulation of a cell-free reaction containing 3 kDa TRITC-Dextran (5 μ M), P70a-S28 (0.2 nM), and P28a-MscL (5 nM) into liposomes via the water-in-oil emulsion transfer method. (B) Fluorescence images of liposomes containing 3 kDa TRITC-dextran over a 2-hour period with only P70a-S28 added to the cell-free reaction. (C) Fluorescence images of liposomes containing 3 kDa TRITC-dextran over a 40-minute period with P70a-S28 and P28a-MscL added to the cell-free reaction. Scale bar: 5 μ m.

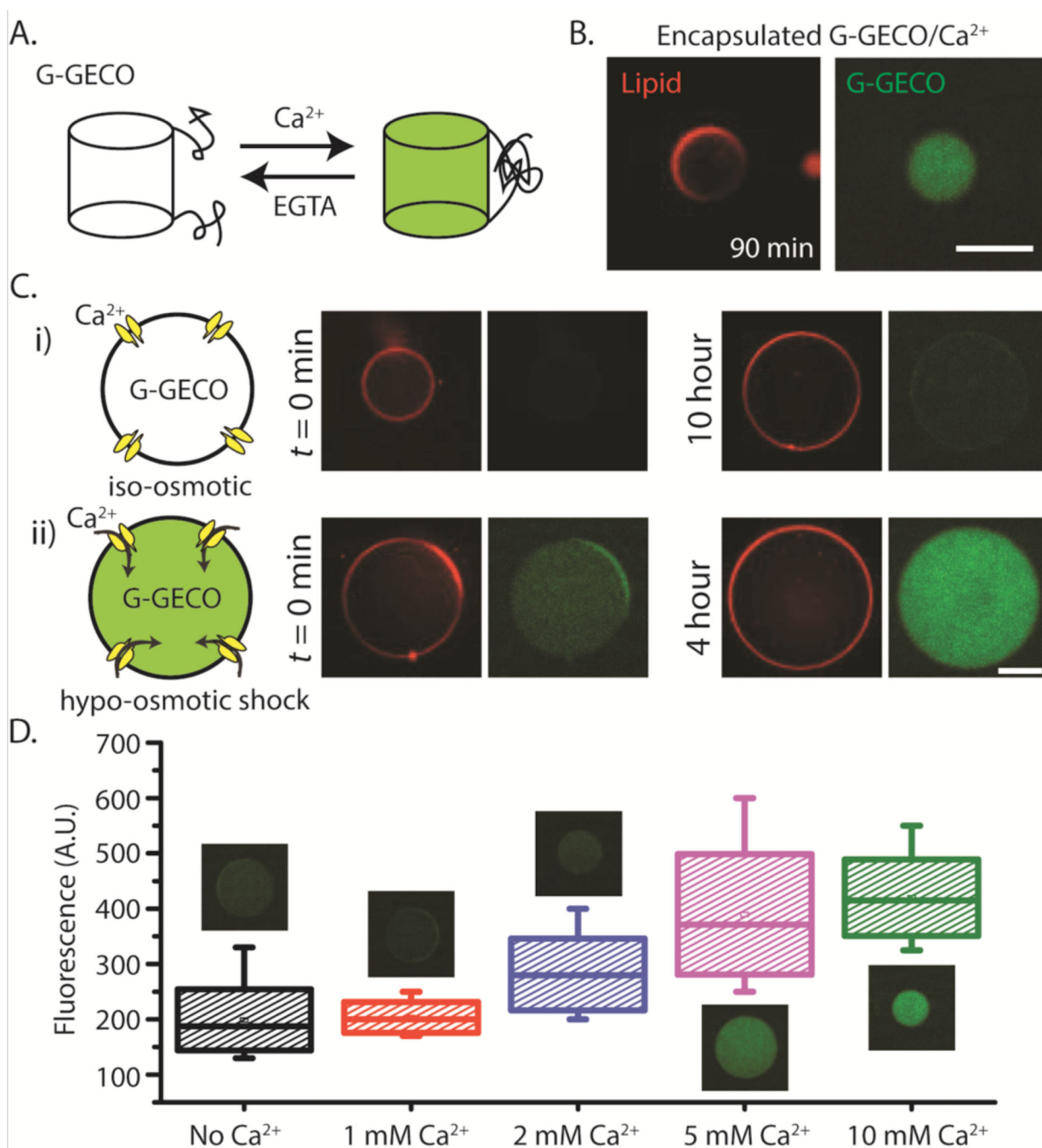


Fig. 4. Mechanosensitive and biosensing synthetic cell system. (A) Schematic depicting the reversible transformation between the fluorescent and non-fluorescent states of G-GECO protein in presence of calcium and EGTA. (B) Fluorescence images of G-GECO expression with calcium addition inside vesicles (1 nM P70a-G-GECO, 1.5 mM calcium chloride was added to TXTL reaction after 1.5 hour incubation prior to encapsulation). (C) (i), (ii)-Three plasmid expression under different external conditions. Concentrations of P70a-S28, P28a-MscL and P70a-G-GECO in cell-free reaction were fixed at 0.2 nM, 1.4 nM and 0.6 nM

respectively. The outer solutions for all conditions contained 10 mM calcium chloride. (D) Box plot showing the relative fluorescence intensities from vesicles in hypo-osmotic media with different external calcium concentrations. Each box corresponds to intensity values from ten vesicles. Plasmid concentrations of P70a-S28, P28a-MscL and P70a-G-GECO were 0.4 nM, 1.3 nM and 1 nM respectively. For both (C) and (D), the lipid vesicles were introduced into hypo-osmotic solution immediately after encapsulation following a 1.5 hour incubation period. EGTA was used at a concentration of 1 mM in all cell-free reactions. The osmolarity difference between iso-osmotic and hypo-osmotic solutions was measured at 100 mOsm. All experiments were repeated three times under identical conditions. Scale bars: 50 μm .